Volume 16, Issue 3, 162520 (1-8)

International Journal of Nano Dimension (IJND)

https://dx.doi.org/10.57647/j.ijnd.2025.1603.20

Exploring the antioxidant, antibacterial and cytotoxicity properties of a green synthesized starch-ascorbic acid-silver nanocomposite

Shabnam Akbari[1], Shiva Khalil-Moghaddam[2,*], Maryam Ghobeh[1], Maryam Bikhof Torbati[2], Ashraf Sadat Shahvelayati[3]

[1]*Departmant of Biology, SR.C., Islamic Azad University, Tehran, Iran.*
[2]*Department of Biology, YI.C., Islamic Azad University,Tehran, Iran.*
[3]*Department of Chemistry, YI.C., Islamic Azad University,Tehran, Iran.*

[*]**Corresponding author:** shiva.moghaddam@yahoo.com

Original Research

Received:
30 October 2024
Revised:
4 December 2024
Accepted:
22 December 2024
Published online:
1 June 2025

Abstract:

This study presents a rapid and efficient synthesis of the starch-silver-ascorbic acid nanocomposite (St-Ag-Asc), that starch and ascorbic acid were used as a stabilizer and reducing agent, respectively. The formation of silver nanoparticles was confirmed through spectrophotometry. The bioactivity of the obtained Nanocomposite(NC) was evaluated by testing the antibacterial, antioxidant, and cytotoxicity activity. Antioxidant activity was tested by the 1,1-diphenyl-2-picrylhydrazyl (DPPH) and ferric-reducing ability of plasma methods. Based on the results of the DPPH test, NC with a half-maximal inhibitory concentration of 0.035 mg/mL demonstrated the high capability in the scavenging of DPPH free radicals. Additionally, as regards the regeneration of ferric iron, the NC (St-Ag-Asc) with a capability of 0.77 mM iron/mg (NC) revealed good regenerative effects against Asc control. Further, minimum inhibitory concentration (MIC) and the Agar well diffusion methods were employed to determine the antibacterial effects. The NC showed antibacterial effects against Escherichia coli, Pseudomonas aeruginosa, and Staphylococcus aureus bacteria with MICs of 0.75 mg/mL, 0.75 mg/mL, and 0.375 mg/mL, respectively. In addition, the cytotoxicity evaluation of the NC by MTT (3-(4,5-dimethylthiazol-2-yl)-2,5-diphenyltetrazolium bromide) assay confirmed its safety toward normal fibroblast cells, indicating its potential use for advanced biomedical applications.

Keywords: Ag nanoparticle; Antibacterial; Antioxidant; Cytotoxicity; Nanocomposite

1. Introduction

For more than a century, severe infections caused by pathogenic bacteria have been the focus of various studies. Although the development of new antibiotics in the past decades has helped humans to treat different infectious diseases, microbial infection treatment has turned into a more complicated issue because bacteria can adapt themselves to antibiotics [1]. For example, *Pseudomonas aeruginosa* (*P. aeruginosa*) causes a wide range of infections of varying severity rates, including pneumonia [2], urinary tract infections [3], and wound infections [4, 5].
Staphylococcus aureus (*S. aureus*) is another type of bacterium that typically colonizes human mucosa and skin and can lead to serious diseases, including bloodstream infection, endocarditis, pneumonia, wound infections, and the like if it enters the body [6]. Likewise, *Escherichia coli* (*E. coli*) is a bacterium that can cause respiratory illnesses, urinary tract infections, wound infections, and pneumonia [7]. It should be mentioned that contamination with microorganisms is a critical factor in various areas, including dental restoration, medical devices, wound healing, food packaging, and so forth [8, 9].
New materials with antibacterial properties are urgently needed, and nanocomposites hold great potential for this purpose [10–12]. Their exceptionally high surface-area-to-volume ratio enhances contact with bacteria, boosting antibacterial effectiveness. Additionally, their unique chemical reactivity and physical properties allow for targeted interactions with bacterial cells, making them highly effective at inhibiting growth. These characteristics position nanocomposites as promising materials for antimicrobial

applications [13].
Recent advancements in the nanotechnology field have enabled the expansion of nano-antibacterial agents such as silver nanoparticles (Ag-NPs), which are considered promising agents with antibacterial effects [14]. Ag-NPs possess attractive biological activities, including antibacterial, antiviral, and antifungal properties, making them vital in preventing various types of infections [15].
At the systemic level, oxidative stress contributes to the advancement and acceleration of various diseases, including cancer, Parkinson's, Alzheimer's, and diabetes. It even plays a role in accelerating aging and reducing the speed of wound healing [16]. To protect against oxidative damage, approximately all organisms have inherent antioxidant defense and repair systems, and such systems are frequently insufficient for complete damage prevention [17]. Hence, it is recommended that antioxidant supplements should be used to decrease oxidative damage to human bodies.
Biomedical substances that have both antioxidant and antibacterial activities are widely used in various industries, such as pharmaceuticals and cosmetics [18]. Of course, the challenge of biocompatibility should not be ignored, and the use of biopolymers such as starch (St) will be useful in this field due to their biodegradability and non-toxicity [19].
In this regard, the researchers of this study synthesized a nanocomposite consisting of three components Ag-NPs, ascorbic acid and St (St-Ag-Asc) with the aim of designing a nanocomposite with antibacterial antioxidant properties using nanoscale science and biological materials. Using the mtt method, the non-toxicity of the resulting nanocomposite was confirmed.

2. Materials and methods

2.1 Materials

All the required chemical reagents were obtained from Sigma Chemical Company. *S. aureus* (ATCC 25923), as a Gram-positive bacterium, as well as *E. coli* (PTCC1399) and *P. aeruginosa* (PTCC1430), as Gram-negative bacteria, were purchased from Pasteur Institute, Tehran, Iran. The BioTeck plate reader (Epoch model, BioTeck Company) was employed to measure light absorbance by samples at varying wavelengths.

2.2 Methods

2.2.1 Synthesis of Nanocomposite

In a typical experiment, $AgNO_3$ (1.69 g) was dissolved in deionized water (50 mL) to create a 100 mM solution. Next, starch (1 g) was added, and the mixture was stirred on a heater-stirrer at 90 °C for 30 minutes, during which a color change from bright yellow to brownish-red was observed. This mixture, referred to as Mix A, was then allowed to cool to room temperature. In a separate container, each of starch and ascorbic acid (0.5 g) were dissolved in deionized water (100 mL) and stirred for 30 minutes at room temperature, forming Mix B. Mix A was added to Mix B under vigorous stirring, resulting in an immediate color change to brown, indicating the successful formation of nanoparticles. The final mixture was centrifuged at 11000 rpm for 5 minutes at 20 °C. The supernatant was carefully removed, while the precipitated pellet was dispersed in phosphate-buffered saline (PBS) [20]. The resulting nanocomposite is referred to as NC (St-Ag-Asc) throughout this text.

2.2.2 Characterization of Ag-NPs

Different techniques were utilized to gather additional data on the size and morphology of Ag-NPs in colloidal suspensions and in NC (St-Ag-Asc) solution [21].

2.2.2.1 UV–Vis spectrophotometry

To track the development of Ag-NPs, ultraviolet-visible (UV-vis) absorption of NC (St-Ag-Asc) was measured using the Perkin Elmer Lambda 750 spectrophotometer at $200-800$ nm [22].

2.2.2.2 FT-IR spectrum

The Spectrum 100 IR spectrometer (BRUKER, TENSOR27) was used with the attenuated total reflectance (ATR) technique for Fourier transform infrared spectroscopy (FTIR) measurements to identify functional groups involved in the synthesis [23].

2.2.2.3 Scanning electron microscopy

The SEM analysis was conducted to characterize the synthesized Ag-NPs particles and determine their shape and size using the (Carl Zeiss Evo 18) model. One milliliter of the sample was used for the analysis.

2.2.3 Evaluation of antioxidant activities

2.2.3.1 The radical scavenging activity of 1,1-diphenyl-2-picrylhydrazyl (DPPH)

In this study, a modified method was utilized to assess DPPH's free radical scavenging ability compared to prior research [24]. In this method, 50 μL of samples at various concentrations were combined with 150 μL of the DPPH solution in a 96-well plate during the testing process. After incubating the microplate for 45 minutes in the dark, the absorbance of the samples was determined at a wavelength of 517 nm. Line equations were derived from inhibition curves. The half-maximal inhibitory concentration (IC_{50}) value was determined by calculating the concentration using the following formula:

$$(\text{A blank} - \frac{\text{A sample}}{\text{A blank}}) \times 100$$

2.2.3.2 Investigation of the ferric reducing antioxidant power (FRAP) technique

This section describes the conversion of the (Fe (III)-TPTZ) complex to (Fe (II)-TPTZ). The FRAP reagent was provided immediately before the experiment using a 300 mM acetate buffer, 10 mM TPTZ, and 20 mM ferrous chloride ($FeCl_3.6H_2O$) in a 10:1:1 ratio. In each well of a 96-cell plate, 20 μL of each sample was merged with 200 μL of the FRAP reagent. The mixture was then mixed on a rotating shaker for 30 minutes at room temperature. The absorption of the samples was determined at 593 nm using a plate reader. The standard curve was plotted using adsorption rates of various ferrous sulfate concentrations ($200-1600$ mM) [25].

2.2.4 Evaluation of the antimicrobial activity

2.2.4.1 Agar well diffusion technique

The intended bacteria were sub-cultured in the Mueller-Hinton broth medium overnight at 37 °C. Then, a 20 mL volume of the medium was poured into a 90-mm-diameter Petri dishes placed on a level surface. After solidifying, bacterial pathogens were swabbed onto agar plates. Three wells with a 5 mm diameter were evenly spaced on the agar per dish. The corresponding concentrations of the St, Asc, and NC (St-Ag-Asc) were added into the respective wells. Next, the Petri dishes were incubated at 37 °C for 24 hours, followed by measuring the diameter of the zone where bacterial growth was inhibited. The means diameters of the inhibition zones were determined as well [26].

2.2.4.2 Estimation of the minimum inhibitory concentration

The antibacterial activity of NC (St-Ag-Asc) was assessed in vitro against several bacterial strains, including Gram-positive bacterium *S. aureus* (ATCC 25923) and Gram-negative bacteria *P. aeruginosa* (PTCC1430) and *E. coli* (PTCC1399).

The MIC values of NC (St-Ag-Asc) were analyzed via broth microdilution in sterile 96-well plates. Aliquots of samples were sequentially diluted in a 96-well plate containing Mueller Hinton Broth (MHB) medium supplemented with 0.5% (v/v) distilled water. The resulting concentration range was 0.0014-6 mg/mL. The bacterial strains were adjusted to 5×10^6 CFU/mL, and the MIC was recorded after incubating 96-well plates at 37 °C for 24 hours. To estimate the minimum bactericidal concentration (MBC), about 100 μL of each well with no growth was spread onto Mueller-Hinton agar and then incubated at 37 °C overnight. The MBC values were reported as the lowest concentrations of NC (St-Ag-Asc) that were able to kill almost all (99.9%) of bacterial cells [27].

2.2.5 Evaluation of cytotoxicity assay

2.2.5.1 Cell culture

Normal fibroblast cells, also known as HFFF2, were cultured in 25-square-centimeter cultivation flasks in a humidified atmosphere containing 5% CO_2 at 37 °C. In addition, Dulbecco's Modified Eagle medium supplemented with a 10% heat-inactivated fetal bovine serum and a high glucose concentration was utilized to achieve the desired population. The cells were detached from the culture flask by adding 0.5 mL of the trypsin solution to phosphate-buffered saline and then incubated for 1 minute at 37 °C [28].

2.2.5.2 MTT assay

The MTT assay was applied to determine the impact of NC (St-Ag-Asc) on cell viability. The cells were exposed to varying concentrations of Ag-NPs (10, 100, 300, and 600 μg/mL) for 24 or 48 hours when they reached 80% confluency. Next, 20 μL of MTT (5 mg/mL) was added to each well at 37 °C for a 4-hour period. Finally, 100 μL of dimethyl sulfoxide was added to each of the wells, and the absorbance was estimated at 570 nm using an ELISA reader [29].

2.2.6 Statistical analysis

All experiments were performed in triplicate. The obtained data are expressed as means ± standard deviations (SD). The results were statistically analyzed by GraphPad Prism software, version 9.2.0. The comparison between the three groups was evaluated using a one-way analysis of variance, followed by Dunnett's multiple comparisons test.

3. Result and discussion

3.1 Characterization

The formation of NC (St-Ag-Asc) was monitored through color change and the maximum absorption peak observed around 430 nm in the UV-Vis absorption spectra. UV-Vis spectroscopy is a reliable technique for confirming the presence of metallic nanostructures. Surface plasmon resonance (SPR), which involves the collective excitation of conduction band electrons near the surface of nanoparticles, plays a key role in this process. After 5 minutes of sonic irradiation, a weak characteristic UV-Vis absorption of silver nanoparticles (Ag-NPs) was detected (figure 1 (a)). Notably, the intensity of the SPR peak at 431 nm increased, further confirming the formation of Ag-NPs [30].

The FT-IR spectra of the Ag-NP samples exhibited multiple peaks, reflecting the complex composition of the biological material (figure 1 (b)). A prominent peak at 3361 cm^{-1} indicates the presence of hydroxyl (O-H) stretching vibrations. Additionally, the band observed around 2073 cm^{-1} suggests the involvement of C-H stretching groups, while the peak at 1637 cm^{-1} may indicate the participation of carboxylic acid (C=O) stretching during the nanoparticle synthesis process. The band at 720 cm^{-1} corresponds to the C-O-C stretching vibrations of glycosidic bonds. Furthermore, the band below 693 cm^{-1} is associated with the formation of metallic silver (Ag). These functional groups in NC (St-Ag-Asc) likely facilitated the reduction of Ag^+ to Ag^0 [31].

The SEM images reveal a complex particulate material with diverse morphological features (figure 1 (c)). Particles range from nanoscale ($30 - 60$ nm) to microscale ($1 - 2$ μm), exhibiting irregular shapes including flaky, angular, and rounded forms. Their surfaces are characteristically rough and layered, often displaying a crumpled or wrinkled texture with numerous protrusions and indentations. The material shows a strong tendency for aggregation, with particles clustering into larger structures. This aggregation, combined with the wide size distribution, indicates a highly polydisperse and heterogeneous sample. Larger particles frequently have smaller ones adhering to their surfaces, contributing to an overall complex texture. The layered structure of many particles suggests a material with a sheet-like molecular arrangement. High-magnification imaging (up to 150000x) provides detailed insights into surface features and precise size measurements, which are crucial for understanding the material's properties and potential applications. This level of structural complexity at both nano and microscales plays a significant role in determining the functional characteristics.

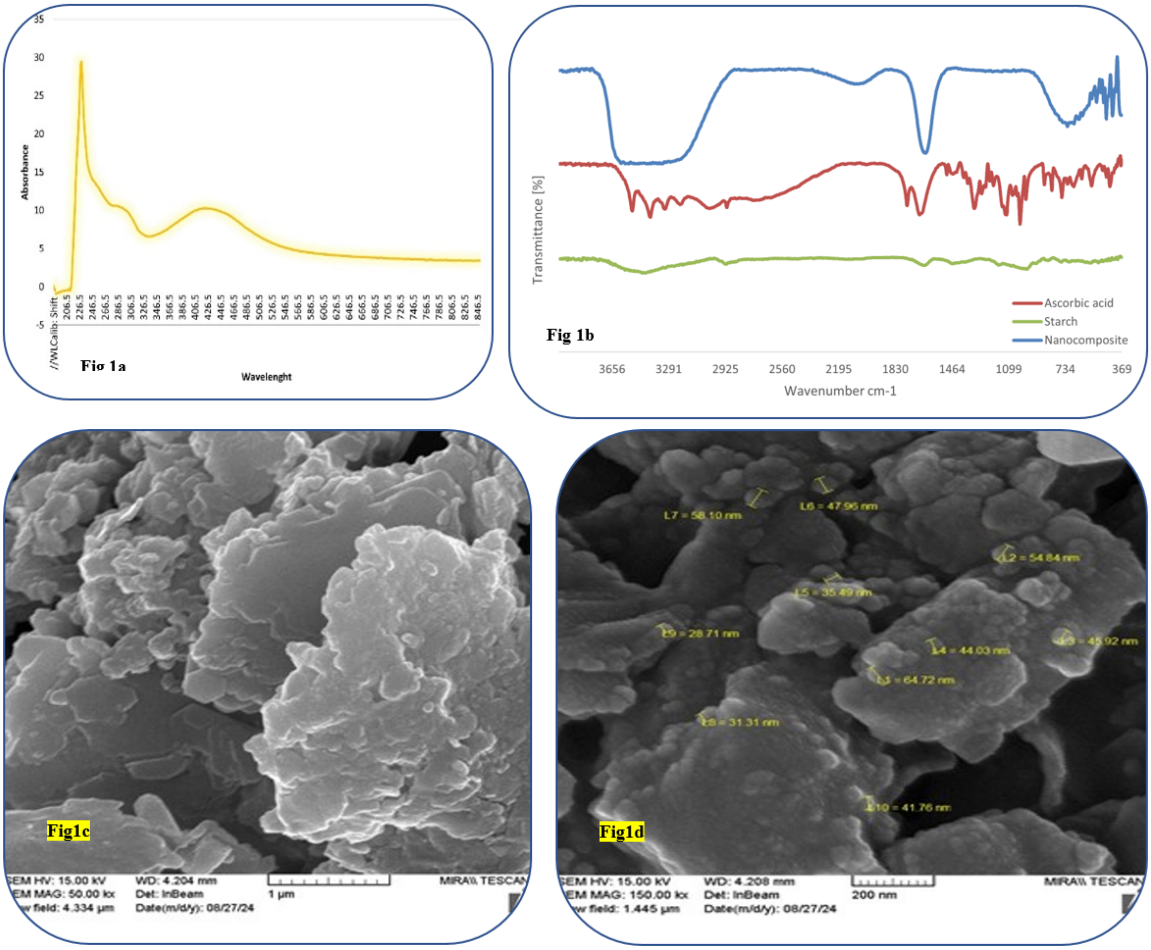

Figure 1. (a) UV-Vis spectra of NC (St-Ag-Asc), (b) FTIR spectrum of NC (St-Ag-Asc), (c) SEM images of NC (St-Ag-Asc) 1 μm, (d) SEM images of NC (St-Ag-Asc) 200 nm .

3.2 Antioxidant activity

The antioxidant activity of NC (St-Ag-Asc) was measured using FRAP and DPPH radical inhibition assays. In the DPPH assay, the reduction of DPPH free radicals indicates the antioxidant effect of the tested sample [32].

Figure 2 (a) compares DPPH radical inhibition at different concentrations of the NC (St-Ag-Asc), starch and ascorbic acid. The linear relationship between the probability of DPPH radical scavenging and the compound concentration was employed to estimate the IC_{50} (Table 1). The IC_{50} value represents the concentration of the sample compound that can scavenge 50% of free radicals in the reaction mixture. According to previous studies, the use of the green synthesis method of Ag-NPs has been related to a noticeable increase in its antioxidant activity [33].

Green synthesized NC (St-Ag-Asc) in the present study showed a significant scavenging DPPH activity with an IC_{50} of 35 μg/mL. This NC at a concentration of 0.37 mg/mL could inhibit 90.96% of free radicals. By increasing the concentration to 3 mg/mL, the rate of free radical inhibition increased to 96.75% (figure 2 (b)). The high antioxidant power of the new NC is probably related to the presence of St and Asc in the green synthesis stages of the NC. Considering that St by itself does not have a high antioxidant effect, it is likely that the presence of Asc in the stages of green synthesis was effective on the high antioxidant power of the NC.

Next, the ferric-reducing ability of NC (St-Ag-Asc) against Asc as the control was investigated at 0.03 mg/mL and 0.3 mg/mL concentrations. This technique utilizes ferric ions (Fe^{3+}) to determine antioxidant power [34]. The data on antioxidant activity with the FRAP assay are shown in figure 2 (c). NC (St-Ag-Asc) demonstrated an increase in the FRAP value with an increase in the concentration from 0.03 mg/mL to 0.3 mg/mL (0.204 ± 0.02 to 0.771 ± 0.03 Fe (II) equivalents (mM)). Our study outcomes are encouraging and provide insights into further investigation of NC (St-Ag-Asc) as a potential antioxidant candidate.

3.3 Antibacterial assessment

The antibacterial activity of NC (St-Ag-Asc) was evaluated against clinical human pathogens, namely, *P. aeruginosa*, *E. coli*, and *S. aureus*, using MIC and MBC assays and the agar well diffusion method. The antibacterial activity of NC (St-Ag-Asc), St, and Asc was determined by the agar well diffusion technique *in vitro*. The zone of inhibition (ZOI) was 17 mm, 20 mm, and 22 mm for *P. aeruginosa*, *E. coli*, and *S. aureus* around the NC (St-Ag-Asc), respectively. Considering that no ZOI was observed around the wells of St and Asc, only Ag in the NC was responsible for the antibacterial effect of the NC (Table 2 a).

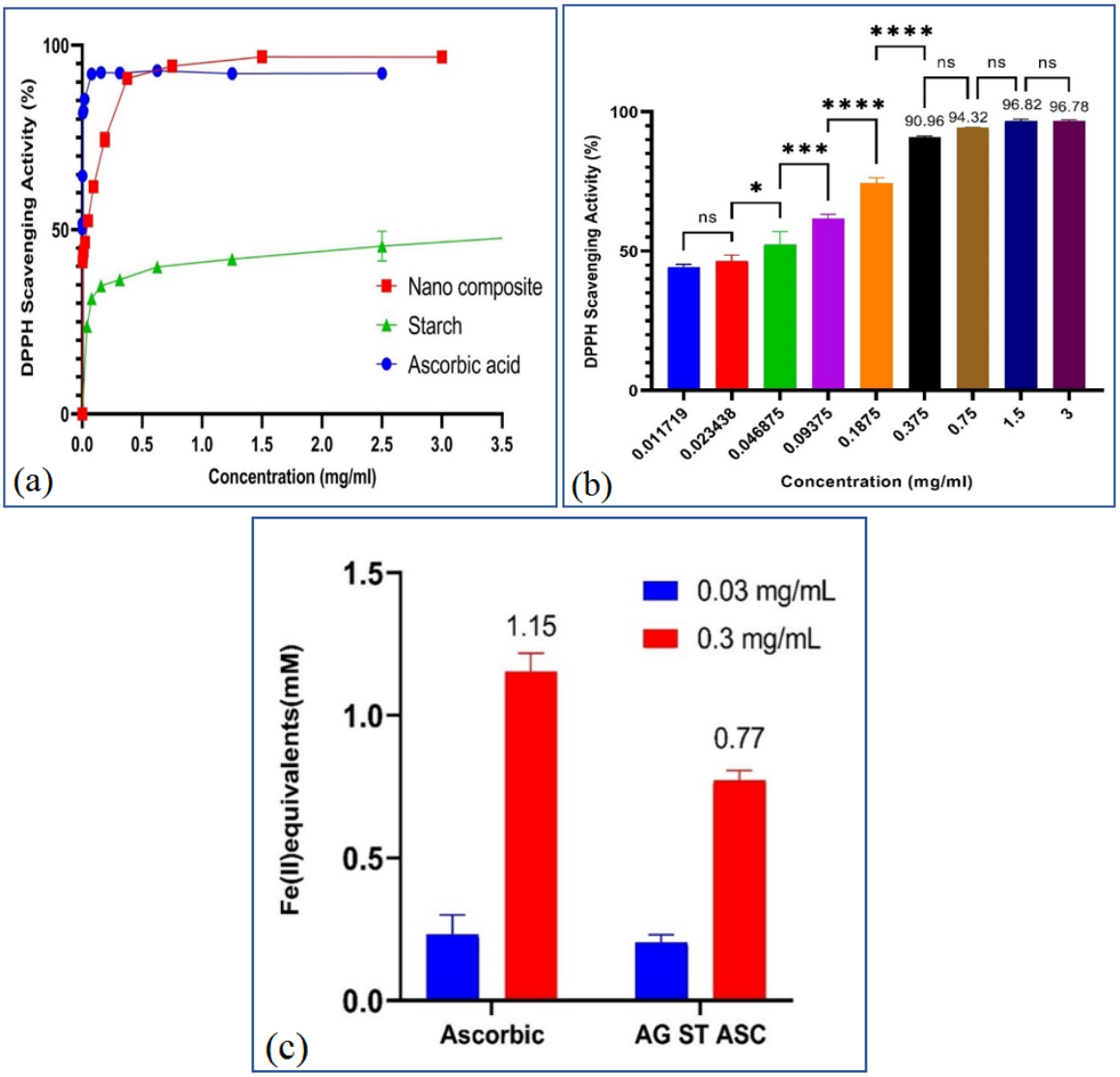

Figure 2. DPPH: 1,1-diphenyl-2-picrylhydrazyl; (a) DPPH radical scavenging activity. NC (St-Ag-Asc): Nanocomposite starch-silver-ascorbic acid; (b) Antioxidant activity of NC (St-Ag-Asc) in different concentration. FRAP: Ferric reducing the ability of plasma; (c) FRAP assay.

Tamara Bruna et al., in their investigation of the antibacterial effect of Ag-NP, reported that Gram-negative bacterial strains had smaller inhibition zones than those of Gram-positive bacterial strains [35], which conforms to the ZOI obtained in this research.The high tendency of Ag to break disulfide bonds was reported in previous studies; probably the disruption of the tertiary structure of cell wall proteins due to the breaking of disulfide bonds and the formation of pits in the membrane structure would be the causes of bacterial death [36].

The bactericidal activity of NC (St-Ag-Asc) was further elucidated using MBC and MIC assays. The MIC values for NC (St-Ag-Asc) were observed at 0.375 mg/mL, 0.75 mg/mL, and 0.75 mg/mL for *S. aureus*, *E. coli*, and *P. aeruginosa*, respectively. NC (St-Ag-Asc) indicated the MBC as 1.5 mg/mL, 1.5 mg/mL, and 3 mg/mL for *S. aureus*, *P. aeruginosa*, and *E. coli*, respectively (Table 2 b). The results confirmed that NC (St-Ag-Asc) could effectively inhibit the growth of bacteria.

Table 1. Antioxidant activity analysis of DPPH assay.

Compound	IC_{50} Value (mg/mL)
Starch	5.880
Ascorbic acid	0.0007
NC (St-Ag-Asc)	0.035

3.4 Cytotoxic studies

Using the MTT assay, cytotoxicity was tested in the HFFF2 cell line (figure 3). This study assessed the activity of mitochondrial dehydrogenase, responsible for converting the MTT reagent from a soluble tetrazole salt to an insoluble formazan [37]. HFFF2 cells were exposed to varying concentrations of NC (St-Ag-Asc) (10 μg/mL, 100 μg/mL, 300 μg/mL, and 600 μg/mL) after 24 and 48 hours of incubation. Based on the results of the MTT assay, no toxicity was observed for fibroblast cells incubated with NC (St-Ag-Asc) at all time points. Meanwhile, the cell proliferation of NC (St-Ag-Asc) exhibited high biocompatibility (figure 3). Our

Table 2. (a) Antibacterial activity of starch, ascorbic acid, and NC (St-Ag-Asc) by the agar diffusion methods.

Microorganisms	Zone of inhibition(mm)		
	Starch	Ascorbic acid	NC (St-Ag-Asc)
E. coli	*	*	20 ± 0.8 mm
P. aeruginosa	*	*	17 ± 0.5 mm
S. aureus	*	*	22 ± 0.4 mm

*(no effective).

Table 2 (b) Antibacterial activity of NC(St-Ag-Asc) and Tetracycline antibiotics by MIC and MBC assays.

Samples	*E. coli*	*P. aeruginosa*	*S. aureus*	
NC(St-Ag-Asc)	MIC (mg/mL)	0.75 mg/mL	0.75 mg/mL	0.375 mg/mL
	MBC (mg/mL)	3 mg/mL	1.5 mg/mL	1.5 mg/mL
Tetracycline	MIC (mg/mL)	0.008 mg/mL	0.032 mg/mL	0.008 mg/mL
	MBC (mg/mL) 0.016 mg/mL	0.128 mg/mL	0.016 mg/mL	

findings revealed that increasing the concentration of NC (St-Ag-Asc) significantly augmented the number of HFFF-2 cells ($p < 0.0001$). Although Ag-NPs had strong antibacterial activity and a wide range of biomedical applications, their cytotoxicity against mammalian cells limited their use as therapeutic agents. Previous studies have shown that Ag-NPs are also toxic to both human skin fibroblasts and keratinocytes [38–41]. However, Starch, as a polymeric material, has been reported to have high biocompatibility while increasing the cell viability of HFFF2. It can absorb NPs and prevent their accumulation by acting as a protective layer and reducing the release of harmful Ag [42]. In the present study, the synthesized NC (St-Ag-Asc) could represent a suitable candidate for biological activities by demonstrating significant antioxidant and antibacterial effects with no toxic effects on fibroblast cells.

4. Conclusion

Nowadays, the use of Ag-NPs in numerous industrial areas is becoming more common. In this research, Ag-NPs were synthesized based on an environmentally friendly and fast method. This new NC has shown significant antioxidant ability, favorable antimicrobial activity, and proliferation effects. In general, the obtained results revealed that NC (St-Ag-Asc) has the potential to be used in different fields, such as medicine, pharmacy, and wound dressing, to stimulate wound healing processes. It is expected that this NC can enter clinics after further optimization studies.

Acknowledgement
We would like to thank the Islamic Azad University, Science and Research Branch, for its spiritual support.

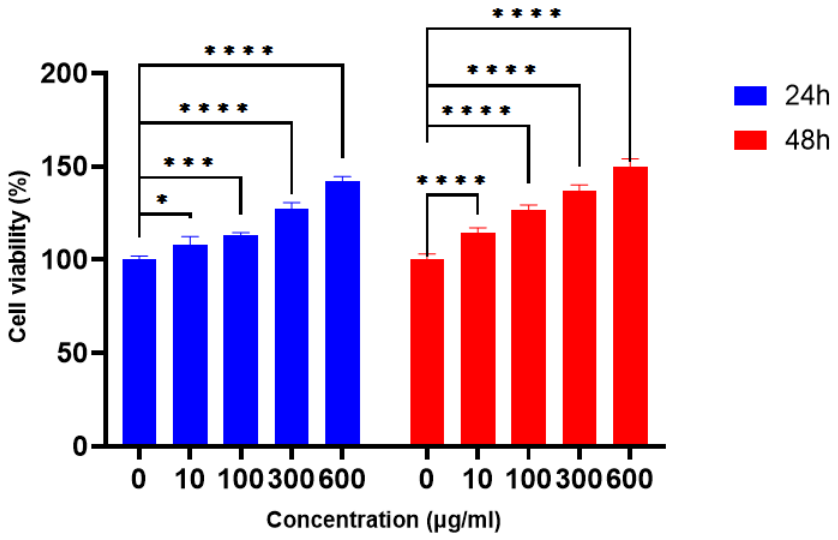

Figure 3. Result of MTT assay of different concentrations of NC (St-Ag-Asc) after 24 and 48 hours. (**** indicates P-value < 0.0001. *** indicates P-value $= 0.0001$)

Authors contributions
Authors have contributed equally in preparing and writing the manuscript.

Availability of data and materials
The authors declare that the data supporting the findings of this study are available within the paper.

Conflict of interests
The authors assert that they do not have any identifiable conflicting financial interests or personal relationships that might be perceived to influence the work presented in this paper.

References

[1] L. Hochvaldova, R. Vecerova, M. Kolar, R. Prucek, L. Kvitek, L. Lapcik, and A. Panacek. "Antibacterial nanomaterials: Upcoming hope to overcome antibiotic resistance crisis.". *Nanotechnol. Rev.*, 11: 1115–1142, 2022.
DOI: https://doi.org/10.1515/ntrev-2022-0059.

[2] G. H. Furtado, P. A. d'Azevedo, A. F. Santos, A. C. Gales, A. C. Pignatari, and E. A. Medeiros. "Intravenous polymyxin B for the treatment of nosocomial pneumonia caused by multidrug-resistant Pseudomonas aeruginosa.". *Int J J. Antimicrob. Agents.*, 30:315–319, 2007.
DOI: https://doi.org/10.1016/j.ijantimicag.2007.05.017.

[3] K. Shigemura, S. Arakawa, S. Sakai, Y.and Kinoshita, K. Tanaka, and M. Fujisawa. "Complicated urinary tract infection caused by Pseudomonas aeruginosa in a single institution (1999-2003).". *Int J Urol.*, 13:538–542, 2006.
DOI: https://doi.org/10.1111/j.1442-2042.2006.01359.x.

[4] M. R. Gonzalez, V. Ducret, S. Leoni, B. Fleuchot, P. Jafari, W. Raffoul, and K. Perron. "Transcriptome analysis of Pseudomonas aeruginosa cultured in human burn wound exudates.". *Front. cell. infect. microbiol.*, 8:39, 2018.
DOI: https://doi.org/10.3389/fcimb.2018.00039.

[5] N. Sathe, P. Beech, L. Croft, C. Suphioglu, A. Kapat, and E. Athan. "Pseudomonas aeruginosa: Infections and novel approaches to treatment "Knowing the enemy" the threat of Pseudomonas aeruginosa and exploring novel approaches to treatment.". *Infectious Medicine*, 2:178–194, 2023.
DOI: https://doi.org/10.1016/j.imj.2023.05.003.

[6] H. Khodadad, F. Hatamjafari, K. Pourshamsian, and B. Sadeghi. "Microwave-assisted Synthesis of Novel Pyrazole Derivatives and their Biological Evaluation as Anti-Bacterial Agents.". *Comb Chem High T Scr.*, 24:695–700, 2021.
DOI: https://doi.org/10.2174/1386207323666201019152206.

[7] X. Wang, Y. Shen, K. Thakur, J. Han, J. G. Zhang, F. Hu, and Z. J. Wei. "Antibacterial Activity and Mechanism of Ginger Essential Oil against *Escherichia coli* and *Staphylococcus aureus*.". *Molecules*, 25:3955, 2020.
DOI: https://doi.org/10.3390/molecules25173955.

[8] I. R. S. Vieira, A. P. A. de Carvalho, and C. A. Conte-Junior. "Recent advances in biobased and biodegradable polymer nanocomposites, nanoparticles, and natural antioxidants for antibacterial and antioxidant food packaging applications.". *Compr. Rev. Food Sci. Food Saf.*, 21:3673–3716, 2022.
DOI: https://doi.org/10.1111/1541-4337.12990.

[9] M. Bagheri, M. Validi, A. Gholipour, P. Makvandi, and E. Sharifi. "Chitosan nanofiber biocomposites for potential wound healing applications: Antioxidant activity with synergic antibacterial effect.". *Bioeng Transl Med.*, 7(1):e10254, 2022.
DOI: https://doi.org/10.1002/btm2.10254.

[10] A. Amininia, K. Pourshamsian, and B. Sadeghi. "Introducing an effective nanocatalytic for the one-pot synthesis and investigation of biological properties of pyranopyrimidinone and xanthene derivatives.". *J. Chil. Chem. Soc.*, 64:4633–4638, 2019.
DOI: https://doi.org/10.4067/S0717-97072019000404633.

[11] H. A. Mohammed, M. A. Amin, G. Zayed, Y. Hassan, M. El-Mokhtar, and M. S. Saddik. "In vitro and in vivo synergistic wound healing and anti-methicillin-resistant Staphylococcus aureus (MRSA) evaluation of liquorice-decorated silver nanoparticles.". *J. Antibiot.*, 76(5):291–30, 2023.
DOI: https://doi.org/10.1038/s41429-023-00603-4.

[12] D. R. Ibraheem, N. G. Alwas, S. H. Abbood, S. M. Nasser, G. M. Sulaiman, M. S. Jabir, and H. A. Fawzi. "Nystatin-Based Zinc Oxide Nanoparticles Coated with Polyethylene Glycol for Enhancing the Antibacterial Activity Against Some Resistance Pathogenic Bacteria.". *BioNanoScience*, pages 1–14, 2024.
DOI: https://doi.org/10.1007/s12668-024-01492-z.

[13] A. Amininia, K. Pourshamsian, and B. Sadeghi. "Nano-ZnO Impregnated on Starch—A Highly Efficient Heterogeneous Bio-Based Catalyst for One-Pot Synthesis of Pyranopyrimidinone and Xanthene Derivatives as Potential Antibacterial Agents.". *Russ. J. Org. Chem.*, 56:1279–1288, 2020.
DOI: https://doi.org/10.1134/S1070428020070234.

[14] E. Esmaeili, T. Eslami-Arshaghi, S. Hosseinzadeh, E. Elahirad, Z. Jamalpoor, S. Hatamie, and M. Soleimani. "The biomedical potential of cellulose acetate/polyurethane nanofibrous mats containing reduced graphene oxide/silver nanocomposites and curcumin: Antimicrobial performance and cutaneous wound healing.". *Int J Biol Macromol.*, 152:418–427, 2020.
DOI: https://doi.org/10.1016/j.ijbiomac.2020.02.295.

[15] J. Siritapetawee, W. Limphirat, P. Pakawanit, and C. Phoovasawat. "Application of Bacillus sp. protease in the fabrication of silver/silver chloride nanoparticles in solution and cotton gauze bandages.". *Biotechnol Appl Biochem.*, 69:20–29, 2022.
DOI: https://doi.org/10.1002/bab.2075.

[16] H. A. Mohammed, G. M. Sulaiman, S. Albukhaty, A. Z. Al-Saffar, F. A. Elshibani, and E. A. Ragab. "Chrysin, The Flavonoid Molecule of Antioxidant Interest.". *ChemistrySelect*, 8:e202303306, 2023.
DOI: https://doi.org/10.1002/slct.202303306.

[17] I. Khalil, W. A. Yehye, A. E. Etxeberria, A. A. Alhadi, S. M. Dezfooli, N. B. M. Julkapli, and A. Seyfoddin. "Nanoantioxidants: Recent Trends in Antioxidant Delivery Applications.". *Antioxidants (Basel)*, 9(1):24, 2019.
DOI: https://doi.org/10.3390/antiox9010024.

[18] T. Munir, A. Mahmood, A. Rasul, M. Imran, and M. Fakhar-e Alam. "Biocompatible polymer functionalized magnetic nanoparticles for antimicrobial and anticancer activities.". *Mater. Chem. Phys.*, 301: 127677, 2023.
DOI: https://doi.org/10.1016/j.matchemphys.2023.127677.

[19] T. Woggum, P. Sirivongpaisal, and T. Wittaya. "Properties and characteristics of dual-modified rice starch based biodegradable films.". *Int. J. Biol. Macromol*, 67:490–502, 2014.
DOI: https://doi.org/10.1016/j.ijbiomac.2014.03.029.

[20] H. Abbasi-Dehnavi and M. Ghashang. "Solvent-free preparation of 3-aryl-2-[(aryl)(arylamino)] methyl-4 H-furo [3, 2-c] chromen-4-one derivatives using ZnO-$ZnAl_2O_4$ nanocomposite as a heterogeneous catalyst. .". *Heterocycl. Commun.*, 24:19–22, 2018.
DOI: https://doi.org/10.1515/hc-2017-0141.

[21] P. Cheviron, F. Gouanve, and E. Espuche. "Green synthesis of colloid silver nanoparticles and resulting biodegradable starch/silver nanocomposites.". *Carbohydr Polym.*, 108:291–298, 2014.
DOI: https://doi.org/10.1016/j.carbpol.2014.02.059.

[22] B. Sadeghi. "Controlled growth and characterization Ag/ZnO nanotetrapods for humidity sensing.". *CCHTS*, 21:462–467, 2018.
DOI: https://doi.org/10.2174/1386207321666180717120417.

[23] M. S. Selvam, P. S. Tresina, G. P. Beulah, and V. R. Mohan. "Phytofabrication of Silver nanoparticles using Abrus precatorius L Seed extract and their antioxidant and antibacterial activity.". *Int. J. Nano Dimens.*, 13:244–255, 2022.
DOI: https://doi.org/10.22034/ijnd.2022.687436.

[24] N. A. Saqa, S. Khalil-Moghaddam, and A. S. Shahvelayati. "DABCO-based ionic liquid-promoted synthesis of indenobenzofurans derivatives: Investigation of antioxidant and antidiabetic activities.". *Heterocycl. Commun.*, 28:164–173, 2022.
DOI: https://doi.org/10.1515/hc-2022-0153.

[25] H. A. Mohammed. "Phytochemical analysis, antioxidant potential, and cytotoxicity evaluation of traditionally used Artemisia absinthium L.(Wormwood) growing in the central region of Saudi Arabia.". *Plants*, 11(8):1028, 2022.
DOI: https://doi.org/10.3390/plants11081028.

[26] M. Prasathkumar, K. Raja, K. Vasanth, A. Khusro, S. Sadhasivam, M. U. K. Sahibzada, and M. S. Elshikh. "Phytochemical screening and in vitro antibacterial, antioxidant, anti-inflammatory, antidiabetic, and wound healing attributes of Senna auriculata (L.) Roxb. leaves.". *Arab. J. Chem.*, 14:103345, 2021.
DOI: https://doi.org/10.1016/j.arabjc.2021.103345.

[27] M. D. Ferreira, L. C. S. Neta, G. C. Brandao, and W. N. L. Dos Santos. "Evaluation of the antimicrobial activity of silver nanoparticles biosynthesized from the aqueous extract of Schinus terebinthifolius Raddi leaves.". *Biotechnol Appl Biochem.*, 70:1001–1014, 2023.
DOI: https://doi.org/10.1002/bab.2415.

[28] L. F. Nie, G. Huang, K. Bozorov, J. Zhao, C. Niu, S. S. Sagdullaev, and H. A. Aisa. "Diversity-oriented synthesis of amide derivatives of tricyclic thieno [2, 3-d] pyrimidin-4 (3 H)-ones and evaluation of their influence on melanin synthesis in murine B16 cells.". *Heterocycl. Commun.*, 24:43–50, 2018.
DOI: https://doi.org/10.1515/hc-2017-0256.

[29] M. Bikhof Torbati, M. Ebrahimian, M. Yousefi, and M. Shaabanzadeh. "GO-PEG as a drug nanocarrier and its antiproliferative effect on human cervical cancer cell line.". *Artif. Cells. Nanomed. Biotechnol.*, 45:568–573, 2017.
DOI: https://doi.org/10.3109/21691401.2016.1161641.

[30] K. Shaw, P. Das, T. Ghorai, T. Chatterjee, S. Gangopadhyay, and S. Mazumder. "fficacy of green synthesis of Silver nanoparticles from Tulsi (Ocimum sanctum) leaf aqueous extract and its antibacterial effect on clinical multidrug-resistant Staphylococcus aureus in West Bengal.". *Int. J. Nano Dimens.*, 14:178–190, 2023.
DOI: https://doi.org/10.22034/ijnd.2023.1975675.2197.

[31] K. Guzman, B. Kumar, M. Grijalva, A. Debut, and L. Cumbal. "Ascorbic Acid-assisted Green Synthesis of Silver Nanoparticles: pH and Stability Study.". *Green Chemistry-New Perspectives*, 2022.
DOI: https://doi.org/10.5772/intechopen.107202.

[32] S. Baliyan, R. Mukherjee, A. Priyadarshini, A. Vibhuti, A. Gupta, R. P. Pandey, and C. M. Chang. "Determination of Antioxidants by DPPH Radical Scavenging Activity and Quantitative Phytochemical Analysis of Ficus religiosa.". *Molecules*, 27:1326, 2022.
DOI: https://doi.org/10.3390/molecules27041326.

[33] N. Eid, N. Yosri, H. R. El-Seedi, H. M. Awad, and H. E. Emam. "Ag@ Sidr honey nanocomposite: chemical profiles, antioxidant and microbicide procurator.". *Biocatal. Agric. Biotechnol.*, 51:102788, 2023.
DOI: https://doi.org/10.1016/j.bcab.2023.102788.

[34] Y. R. Girish, K. S. Sharath Kumar, K. Prashantha, S. Rangappa, and M. S. Sudhanva. "Significance of antioxidants and methods to evaluate their potency.". *Mater Chem Horizons*, 2:93–112, 2023.
DOI: https://doi.org/10.22128/mch.2023.647.1037.

[35] T. Bruna, F. Maldonado-Bravo, P. Jara, and N. Caro. "Silver nanoparticles and their antibacterial applications.". *Int. J. Mol. Sci.*, 22:7202, 2021.
DOI: https://doi.org/10.3390/ijms22137202.

[36] R. Asamoah, E. Annan, B. Mensah, P. Nbelayim, V. Apalangya, B. Onwona-Agyeman, and A. Yaya. "A comparative study of antibacterial activity of CuO/Ag and ZnO/Ag nanocomposites.". *Adv. Mater. Sci. Eng.*, 2020:7814324, 2020.
DOI: https://doi.org/10.1155/2020/7814324.

[37] S. Kudłacik-Kramarczyk, A. Drabczyk, M. Głąb, D. Alves-Lima, H. Lin, T. Douglas, and B. Tyliszczak. "Investigations on the impact of the introduction of the Aloe vera into the hydrogel matrix on cytotoxic and hydrophilic properties of these systems considered as potential wound dressings.". *Mater. Sci. Eng. C*, 123:111977, 2021.
DOI: https://doi.org/10.1016/j.msec.2021.111977.

[38] N. Amiri, S. Ghaffari, I. Hassanpour, T. Chae, R. Jalili, R. Kilani, and D. Lange. "Antibacterial Thermo-Sensitive Silver Hydrogel Nanocomposite Improves Wound Healing.". *Gels.*, 9:542, 2023.
DOI: https://doi.org/10.3390/gels9070542.

[39] A. Galandakova, J. Frankova, N. Ambrozova, K. Habartova, V. Pivodova, B. Zalesak, and J. Ulrichova. "Effects of silver nanoparticles on human dermal fibroblasts and epidermal keratinocytes.". *Hum Exp Toxicol.*, 35:946–957, 2016.
DOI: https://doi.org/10.1177/0960327115611969.

[40] M. Paknejadi, M. Bayat, M. Salimi, and V. Razavilar. "Concentration- and time-dependent cytotoxicity of silver nanoparticles on normal human skin fibroblast cell line.". *IRCMJ.*, 20:1–8, 2018.
DOI: https://doi.org/10.5812/ircmj.79183.

[41] C. V. Vivas, J. A. dos Santos, Y. B. Barreto, S. H. Toma, J. J. dos Santos, M. A. Stephano, and A. C. Bloise. "Biochemical response of human endothelial and fibroblast cells to silver nanoparticles.". *J. Bionanosci.*, 13:502–520, 2023.
DOI: https://doi.org/10.1007/s12668-023-01091-4.

[42] K. Saravanakumar, B. Sriram, A. Sathiyaseelan, A. V. A. Mariadoss, X. Hu, K. S. Han, and M. H. Wang. "Synthesis, characterization, and cytotoxicity of starch-encapsulated biogenic silver nanoparticle and its improved anti-bacterial activity.". *Int J Biol Macromol.*, 182: 1409–1418, 2021.
DOI: https://doi.org/10.1016/j.ijbiomac.2021.05.036.